Structure and spectroscopic properties of [di(3-aminopropyl)amine-*N,N',N''*][iminodiacetato-*N,O,O'*]chromium(III) perchlorate

Vaseetha Subramaniam, Kyu-Wang Lee* and Patrick E. Hoggard**
Department of Chemistry, North Dakota State University, Fargo, ND 58105 (USA)

(Received June 25, 1993; revised September 25, 1993)

Abstract

The mixed-ligand complex $[Cr(dpt)(ida)]ClO_4 \cdot 2H_2O$ (dpt = di(3-aminopropyl)amine, H_2ida = iminodiacetic acid) adopts a structure in which the ligands are tridentate and coordinate facially, with the imino nitrogen *trans* to the dpt secondary amine. Thus the preference of iminodiacetate for facial coordination prevails over the preference of di(3-aminopropyl)amine for meridional coordination. The crystal structure of the title complex has been determined: space group *Pbca*; $a = 17\,609(2)$, $b = 14.762(2)$, $c = 14\,423(2)$ Å, $Z = 2$. An analysis of the $^4A_{2g} \rightarrow \{^2E_g, {}^2T_{1g}\}$ electronic spectrum shows the iminodiacetate carboxylate groups to be moderately strong σ- and π-donors.

Key words: Crystal structures; Chromium complexes, Chelate ligand complexes; Amine complexes

Introduction

Many tridentate ligands have a strong preference for facial or meridional coordination, and thus dictate the geometry of a complex formed from one such ligand and one or more additional ligands. Most tridentate amino acids, for example, coordinate facially [1, 2], while glycylglycine coordinates meridionally [3, 4]. Each enforces its stereochemistry on diethylenetriamine, which does not have a strong preference [5, 6]. Di(3-aminopropyl)amine (dpt) has a moderately strong preference for meridional coordination [7, 8], strong enough in fact to force the amino acid lysine (Hlys) into meridional coordination in $[Cr(dpt)(L\text{-lys})]^{2+}$ [9]. Iminodiacetic acid has a moderate preference for facial coordination [10], though there are a few instances of meridional coordination [11, 12]. One of the objectives of the work reported in this paper was to synthesize the mixed-ligand complex $[Cr(dpt)(ida)]^+$, in order to see which ligand can enforce its preferred stereochemistry on the other.

A second objective was to determine the ligand field properties of the iminodiacetate ligand, both the carboxylate and the imino groups, in terms of the angular overlap model (AOM) parameters e_σ and e_π. The method we employ requires the identification of several of the sharp-line $^4A_{2g} \rightarrow \{^2E_g, {}^2T_{1g}\}$ transitions [13]. All but one or two of these have proved difficult to identify and assign properly in the spectrum of salts of $[Cr(ida)_2]^-$ [14, 15].

Experimental

Iminodiacetic acid and di(3-aminopropyl)amine were obtained from Aldrich. *mer*-$[Cr(dpt)Cl_3]$ was synthesized by the method of House and Robinson [7a].

$[Cr(dpt)(ida)]ClO_4 \cdot 2H_2O$

Iminodiacetic acid (0.84 g; 0.0050 mol) was added to a suspension of $[Cr(dpt)Cl_3]$ (1.44 g; 0.0050 mol) in methanol (75 ml). The mixture was heated in a water bath maintained at 50 °C for 1 h with occasional stirring. KOH (0.56 g; 0.020 mol) was then added and heating was continued until the $[Cr(dpt)Cl_3]$ was completely dissolved. A red–violet precipitate of $K[Cr(ida)_2]$ formed, which was filtered off and discarded. The red–orange filtrate was left at room temperature for several hours. A water-soluble orange solid deposited and was separated by filtration. It was recrystallized by dissolving in a minimum amount of water, then adding $LiClO_4$ until the orange precipitate reformed. The precipitate was dissolved again by heating the solution, then a saturated solution of $LiClO_4$ in ethanol

*Present address. Department of Chemistry, Myong-Ji University, Yong-In, Kyonggi-Do 449-728, Korea.
**Author to whom correspondence should be addressed.

SSDI 0020-1693(93)03722-M

was added until precipitation began. The solution was cooled, and crystals were collected by filtration, washed with ethanol, and air-dried. **Caution**: Though no problems were experienced, with perchlorate salts appropriate safeguards should be taken against the possibility of explosion.

IR spectra were recorded on a Mattson Cygnus-25 FTIR spectrometer on samples dispersed in KBr discs. UV–Vis absorption spectra were measured with a Hewlett-Packard model 8451A diode array spectrometer Luminescence and excitation spectra were recorded with an apparatus consisting of a PAR Dyescan nitrogen laser-pumped dye laser source, a Spex 1672 double 220 mm monochromator, and a SRS boxcar averager. Microcrystalline samples were mounted with conductive grease on the cold head of an Air Products closed-cycle He gas cryostat. Excitation spectra were recorded by scanning over the range of one or more dyes, and the output signals were corrected for the variation in laser intensity by dividing by the signal from a small portion of the beam passing through the rear mirror into a fiber optic cable.

X-ray diffraction data were collected by the Molecular Structure Corporation on a Rigaku AFC6R diffractometer equipped with a graphite crystal incident beam monochromator. An orange, prismatic crystal of $[Cr(dpt)(ida)]ClO_4 \cdot 2H_2O$, having the approximate dimensions $0.30 \times 0.30 \times 0.30$ mm, was mounted on a glass fiber. Cell constants and an orientation matrix for data collection were obtained from a least-squares refinement, using the setting angles of five carefully centered reflections in the range $30.04 < 2\theta < 35.18°$. The orthorhombic cell parameters and specific data collection parameters are shown in Table 1.

The structure was solved by conventional direct methods [16], and all non-hydrogen atoms were refined anisotropically. The structure was refined by a full-matrix least-squares method, in which the function minimized was $\Sigma w(|F_o| - |F_c|)^2$ was used for the refinement. The refinement used a sigma weighting scheme ($w = 1/\sigma^2(F)$), and reached a final R value of 0.067 ($R_w = 0.089$). Details are given in Table 1. All calculations were performed with the Texsan crystallographic package, obtained from the Molecular Structure Corporation.

$[Cr(dpt)(ida)]ClO_4 \cdot 2H_2O$ was dissolved in water and the solution was loaded onto a Sephadex SP cation exchange column. It was eluted as a single band with 0.3 M $NaClO_4$, which we have found empirically to be consistent with a +1 charge on the complex. The molar conductivity in water was 77 ohm^{-1} cm^2 mol^{-1}, again consistent with a 1:1 electrolyte.

TABLE 1 Experimental and data processing parameters for X-ray diffraction study of di(3-aminopropyl)amine(iminodiacetato)chromium(III) perchlorate

Crystal data	
$[Cr(dpt)(ida)]ClO_4$ $2H_2O$	$CrC_{10}H_{26}ClN_4O_{10}$
Formula weight	449 79
Crystal dimensions (mm)	$0\ 30 \times 0\ 30 \times 0\ 30$
Peak width at half height	0.35
Radiation	MoKα
Temperature (°C)	23
Space group	orthorhombic *Pbca* (No 61)
a (Å)	17 609(2)
b (Å)	14 762(2)
c (Å)	14 423(2)
V (Å^3)	3749
Z	8
D_{calc} (g/cm^3)	1 594
Linear absorption coefficient (cm^{-1})	7.9
Intensity measurements	
Diffractometer	Rigaku AFC6R
Monochromator	graphite crystal, incident beam
Take-off angle (°)	6.0°
Detector aperture (mm)	6.0 horizontal and vertical
Crystal detector distance (cm)	40 cm
Scan type	ω–θ
Scan width	$1\ 15 + 0\ 30 \tan \theta$
Scan rate	32 0/min (in omega)
Maximum 2θ	50
No reflections measured	3726
Corrections	Lorentz polarization
Solution	direct methods
Refinement	full-matrix least-squares
Minimization function	$\Sigma w(\|F_o\| - \|F_c\|)^2$
Least-squares weight	$4F_o^2/\sigma^2(F_o^2)$
Anomalous dispersion	all non-hydrogen atoms
Reflections included	1772
Parameters refined	304
Unweighted agreement factor	0 068
Weighted agreement factor	0.089
E.s d. of observation of unit weight	3 02
Highest peak in final diffraction map (e$^-$/Å^3)	0 65
Goodness of fit	2 76
Maximum shift/error	0.01

Results and discussion

Structure

Two facial isomers and one meridional isomer are possible, see Fig. 1. A PCMODEL [17] molecular mechanics calculation was undertaken to predict which isomer would be most stable. PCMODEL is based on the MMX force field [18], and omits force constants for ligand–metal–ligand angle bending, relying on van der Waals forces to achieve the proper angles. The total MMX energy consists of the strain energy (from bond stretching, angle bending, torsional, and van der Waals forces) plus a dipole–dipole energy to account

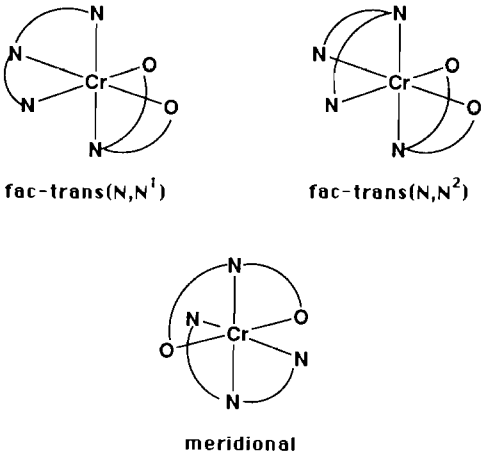

Fig 1. Geometric isomers of $[Cr(dpt)(ida)]^+$

TABLE 2 Molecular mechanics energies (kJ/mol) calculated by PCMODEL for isomers of $[Cr(dpt)(ida)]^+$

Isomer	Strain energy	Dipole–dipole energy	Total energy
PCMODEL force field			
fac-trans(N,N¹)	103	−20	83
fac-trans(N,N²)	107	−19	88
meridional	105	−28	77
PCMODEL force field + L-M-L constants[a]			
fac-trans(N,N¹)	99	−52	47
fac-trans(N,N²)	84	−50	34
meridional	85	−48	37

[a] $k_b = 0.30$ mdyne Å rad^{-2} around $\theta_0 = 90°$ and 180° [20], all r_0(M–L) values 0.15 Å longer (Cr–N, 2.13, Cr–O, 1.95 Å).

for electrostatic contributions in a polar molecule. Calculations were performed from several initial geometries to try to ensure that the global minimum was found.

Table 2 shows the calculated energies after geometry optimization for the three isomers (notation: N, ida nitrogen; N^1, primary dpt nitrogen; N^2, secondary dpt nitrogen). The meridional isomer had the lowest energy, but by an amount too small to have predictive value. The calculations were repeated after increasing r_0, the strain-free bond distance, for the metal–ligand bonds, and adding ligand–metal–ligand bending force constants of 0.30 mdyne Å rad^{-2}. This altered the relative energies sufficiently that the facial-*trans*(N,N^2) isomer was lowest, but still not by enough to make a firm prediction.

Figure 2 shows the UV–Vis spectrum of $[Cr(dpt)(ida)]^+$. The first spin-allowed band, representing the $^4A_{2g} \rightarrow {}^4T_{2g}$ transition in octahedral notation, has a maximum at 486 nm with an extinction coefficient of 59 M^{-1} cm^{-1}. This is typical of meridional dpt complexes of Cr(III) with a variety of other ligands [7], though the spectra of $[Cr(dpt)L]^+$ complexes, where L is a planar tridentate ligand such as a dipeptide,

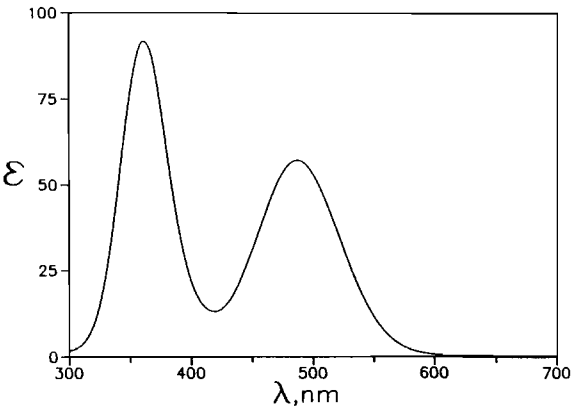

Fig 2 UV–Vis spectrum of $[Cr(dpt)(ida)]^+$ in aqueous solution at 24 °C.

have much higher first band extinction coefficients, typical of all complexes with such ligands [3, 4]. The UV–Vis spectrum cannot be used to infer meridional coordination, however, for lack of facial dpt complexes of Cr(III) with which to compare it.

The IR spectral data are listed in Table 3. The asymmetric carboxylate stretching band at 1636 cm^{-1} confirms coordination of the ida carboxylate groups [19]. Schmidtke and Garthoff have identified several features diagnostic of meridional coordination in transition metal complexes of diethylenetriamine (dien) [6], which may be presumed also to be valid for di(3-aminopropyl)amine complexes [20]. One or two bands associated with an NH_2 rocking motion appear between 700 and 800 cm^{-1} for facial isomers, but two bands occur instead near 850 cm^{-1} for meridional isomers [6]. In the $[Cr(dpt)(ida)]ClO_4 \cdot 2H_2O$ spectrum there are two bands (703 and 790 cm^{-1}) A band near 1250 cm^{-1}, associated with an NH wagging motion by Schmidtke and Garthoff [6], is found for meridional but not for facial isomers. It is absent in the spectrum of $[Cr(dpt)(ida)]ClO_4 \cdot 2H_2O$. An N–H stretching band was found by Yoshikawa and Yamasaki near 2850 cm^{-1} in meridionally coordinated dien complexes [21], but does not occur in this spectrum. All of these features are consistent with facial coordination of dpt (and thus of ida), though they do not enable us to distinguish between the two facial isomers. This led us to perform a molecular structure determination from single crystal X-ray diffraction data.

Description of X-ray structure

A perspective ORTEP drawing of the $[Cr(ida)(dpt)]^+$ cation is shown in Fig. 3, together with the numbering scheme. The fractional coordinates are shown in Table 4 and the bond distances and angles are summarized in Table 5. The chromium atom is surrounded by two oxygens and four nitrogens, in the facial-*trans*(N,N^2) orientation. The dpt coordination geometry is not greatly

TABLE 3 Relevant frequencies and assignments from the IR spectra of $[Cr(dpt)(ida)]ClO_4\ 2H_2O$, *mer*-$[Cr(dpt)(glygly)]ClO_4$ and *mer*-$[Cr(dpt)(L\text{-}lys)]Cl_2$ ($H_2glygly$ = glycylglycine, Hlys = lysine)

$[Cr(dpt)(ida)]ClO_4$	*mer*-$[Cr(dpt)(glygly)]ClO_4$[a]	*mer*-$[Cr(dpt)(L\text{-}lys)]Cl_2$[a]	Assignment
	2885	2865	ν(N–H) amine
1636	[b]	1635	$\nu_{as}(CO_2)$
	1576	1576	$\delta(NH_2)$ dpt
1282			$\omega(NH_2)$ dpt
	988	985	dpt
952			ida
	912	913	dpt
919			ida
901			ida

[a]Ref. 9 [b]Obscured by imide ν(C=O) band.

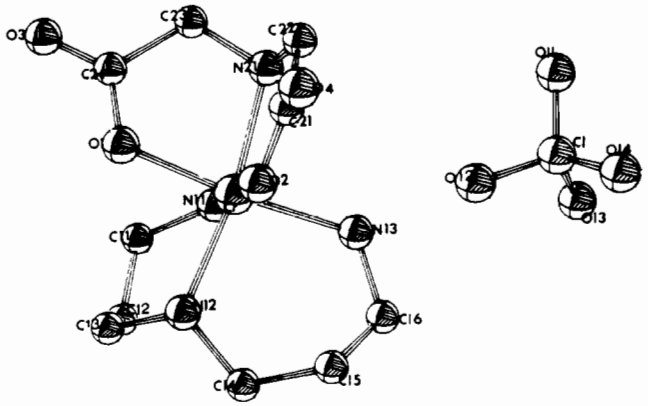

Fig 3 ORTEP drawing of $[Cr(dpt)(ida)]ClO_4 \cdot 2H_2O$

distorted from octahedral, and the Cr–N bond lengths are similar to those in 1,3-propanediamine complexes of chromium(III) [22].

The crystal structure confirms that iminodiacetic acid is not coordinated meridionally, even though the synthesis was initiated with meridionally coordinated di(3-aminopropyl)amine in $[Cr(dpt)Cl_3]$. This indicates that, contrary to our expectation, iminodiacetic acid has a stronger tendency to coordinate facially to chromium(III) than di(3-aminopropyl)amine does to coordinate meridionally.

Spectroscopy

The 13 K luminescence spectrum of $[Cr(dpt)(ida)]ClO_4 \cdot 2H_2O$ is shown in Fig. 4, and is typical of ^2E_g emission in chromium(III) complexes. The lower energy $^2E_g \rightarrow {}^4A_{2g}$ electronic origin (R_1) was observed at 14 330 cm^{-1}. The two bands at higher energy had intensities that were independent of temperature, and therefore do not result from emission from a higher electronic or vibronic state in the same complex. It is possible that a phase transition occurs at low temperature, leading to inequivalent chromium sites. If so, the luminescence intensities of higher energy sites would be approximately equivalent to the intensity of the lowest energy site if there was no transfer of excitation energy between sites. If excitation energy transfer were complete, higher energy sites would have no associated luminescence intensity. The spectrum in Fig. 4 could represent an intermediate situation. It is also possible that they represent impurity emission or defect sites. Table 6 lists the observed peak positions.

The 13 K excitation spectrum in the $^4A_{2g} \rightarrow \{^2E_g, {}^2T_{1g}\}$ region (Figs. 5 and 6) was recorded by monitoring the vibronic peak at 14 246 cm^{-1} in the luminescence spectrum while scanning the dye laser frequency. The

TABLE 4. Fractional coordinates and isotropic thermal parameters for $[Cr(dpt)(ida)]ClO_4\ 2H_2O$

Atom	x	y	z	B_{eq}[a]
Cr	0 44660(8)	0 6456(1)	0.3888(1)	2.36(6)
Cl	0 3374(2)	0 9427(2)	0 5443(2)	4.1(1)
O1	0.4286(3)	0.5147(4)	0 3958(4)	2.6(3)
O2	0 4256(4)	0 6575(5)	0 5201(5)	3.8(4)
O3	0 3518(4)	0 4035(5)	0 3542(6)	4.6(4)
O4	0.3373(6)	0 6629(6)	0 6303(6)	7.6(6)
O11	0 3726(7)	0.9929(8)	0.4713(8)	10.2(8)
O12	0.3770(9)	0 8863(8)	0 5585(9)	12.0(1)
O13	0.337(1)	0 992(1)	0 621(1)	16.0(1)
O14	0 2674(8)	0 925(1)	0 517(1)	16.0(1)
O21	0 7359(7)	0.2918(7)	0.2156(7)	10.9(7)
O22	0 0107(6)	0 6848(5)	0 8149(5)	6.4(5)
N11	0 4683(4)	0 6366(5)	0.2481(6)	3.3(4)
N12	0 5601(5)	0.6248(5)	0.4201(6)	3.3(4)
N13	0 4536(5)	0 7860(5)	0 3797(6)	3.8(4)
N21	0.3280(4)	0.6445(6)	0.3785(7)	4.0(4)
C11	0.5198(7)	0.5635(7)	0.2166(8)	4.3(6)
C12	0 5969(7)	0 5677(7)	0.2620(9)	5.0(7)
C13	0.5970(6)	0.5531(8)	0.3670(9)	4.3(6)
C14	0.6102(7)	0 7049(8)	0.427(1)	5.6(7)
C15	0.572(1)	0 788(1)	0.466(1)	7.0(1)
C16	0 5203(8)	0.8356(8)	0.411(1)	5.4(7)
C21	0.3552(8)	0 6624(7)	0.549(1)	5.0(7)
C22	0 2973(7)	0 6647(7)	0.472(1)	4 8(7)
C23	0 3052(6)	0.5538(8)	0.3442(8)	3.9(5)
C24	0.3653(6)	0 4837(7)	0.3640(7)	3.0(5)

[a]For anisotropic thermal parameters see ref 9.

TABLE 5. Bond lengths and bond angles in [Cr(dpt)(ida)]-ClO_4 $2H_2O$

	X-ray	PCMODEL[a]	PCMODEL[b]
Bond lengths (Å)			
Cr–N11	2 069(9)	1.911	2 058
Cr–N12	2.073(8)	1 921	2 067
Cr–N13	2 080(8)	1 930	2.069
Cr–N21	2.094(8)	1.961	2.066
Cr–O1	1.961(6)	1.853	1 968
Cr–O21	1.938(7)	1 849	1.958
Bond angles (°)			
O1–Cr–O2	90 5(3)	83.0	83.8
O2–Cr–N11	178.4(3)	175.4	177.0
O2–Cr–N12	89.1(3)	87 1	88.8
O2–Cr–N13	89 0(3)	92 9	91.3
O2–Cr–N21	83 1(4)	85.2	85.0
O1–Cr–N11	90.9(3)	96 6	94 0
O1–Cr–N12	89.9(3)	91 4	90.4
O1–Cr–N13	174 0(3)	168.6	173.8
O1–Cr–N21	80.5(3)	83.8	88 5
N12–Cr–N11	91 5(3)	97.5	93 1
N12–Cr–N13	96 0(3)	99 1	93.3
N12–Cr–N21	167 6(3)	171 4	173.9
N11–Cr–N13	89 5(3)	86.8	90.8
N11–Cr–N21	93 6(4)	97 5	92.9
N13–Cr–N21	93 6(3)	85 3	87.3

E.s.d.s. in the least significant figure in parentheses [a]Unmodified [b]With force field alterations listed in Table 2

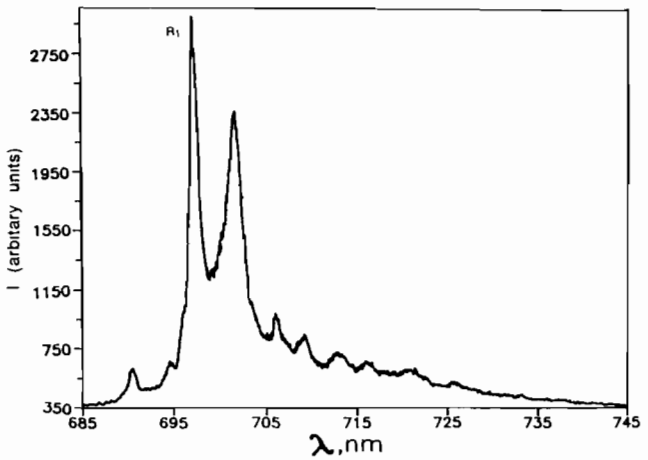

Fig. 4 13 K luminescence spectrum of $[Cr(dpt)(ida)]ClO_4 \cdot 2H_2O$.

spectrum was unchanged when other vibronic peaks were used. The assignment of the five electronic origins in this spectral region was made by examining each peak as a possible origin and choosing those for which remaining lines could be assigned to a pattern of vibronic sidebands that showed consistency among the chosen electronic origins and also with the luminescence spectrum. This complex has no symmetry, and thus there are no overt selection rules, which can alter the vibronic patterns to be expected with different electronic origins. The assignment of the observed lines is shown in

TABLE 6. Vibronic intervals in the 13 K luminescence spectrum of $[Cr(dpt)(ida)]ClO_4 \cdot 2H_2O$ (cm^{-1})

$14330 - \tilde{\nu}$	Assignment	$14330 - \tilde{\nu}$	Assignment
−147m		320m	
−61m		340w	
0vs	R_1	367w	
84vs		403w	
174m		461w	ν(Cr–O)
192w		471w	ν(Cr–N)
220w		494w	
239m		556w	
308m			

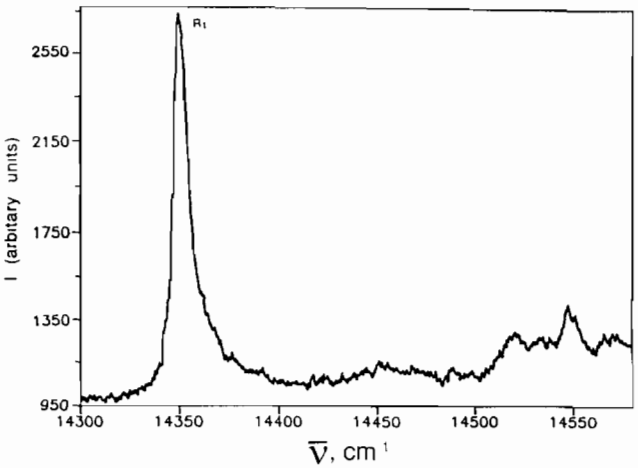

Fig. 5 13 K excitation spectrum of $[Cr(dpt)(ida)]ClO_4 \cdot 2H_2O$ in the region 14 300–14 550 cm^{-1}

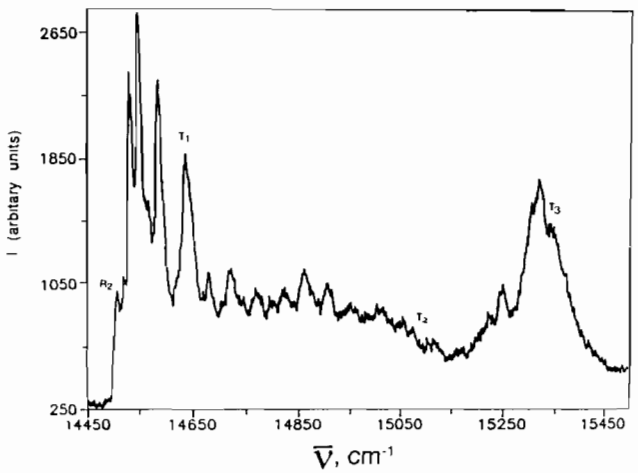

Fig 6. 13 K excitation spectrum of $[Cr(dpt)(ida)]ClO_4 \cdot 2H_2O$ in the region 14 450–15 450 cm^{-1}.

Table 7. The $^4A_{2g}$ transition labeled T_2 was less certain than the others, because of the inverted intensity relationship with its assigned vibronic satellites.

The methods have been described previously by which transition energies can be calculated by evaluating the

TABLE 7 Peak positions and assignments in the 13 K sharp-line excitation spectrum of [Cr(dpt)(ida)]ClO_4 $2H_2O$ (all data in cm^{-1})

$14353-\tilde{\nu}$	Assignment	Vibronic frequencies	Ground state frequencies[a]
0vs	R_1	ν_1 85	85
85	$R_1+\nu_1$	ν_2 187	176
156ms	R_2	ν_3 197	199
167ms		ν_4 218	220
187vs	$R_1+\nu_2$	ν_5 239	239
197vs	$R_1+\nu_3$	ν_6 332	340
218s	$R_1+\nu_4$		
239vs	$R_1+\nu_5$		
290s	T_1		
332m	$R_1+\nu_6$		
353m	$R_2+\nu_3$		
394w	$R_2+\nu_5$		
415m	$R_1+\nu$(Cr–O)		
467mw	$R_1+\nu$(Cr–N)		
477w	$T_1+\nu_2$		
508vw			
529w	$T_1+\nu_5$		
560m			
602w			
653w			
768m	T_2		
809			
871			
902ms			
954s	$T_2+\nu_2$		
975vs	$T_2+\nu_5$		
992s	T_3		

[a]From the luminescence spectrum (Table 6).

TABLE 8 Cartesian coordinates for ligating atoms in [Cr(dpt)(ida)]ClO_4 $2H_2O$[a]

Atom[b]	x	y	z
O1	−0.317	−1.932	0.101
O2	−0.370	0.176	1.894
N21	−2.088	−0.016	−0.149
N11	0.382	−0.133	−2.029
N13	0.123	2.073	−0.131
N12	1.999	−0.307	0.451
C	−1.432	−2.390	−0.358
C	−1.609	0.248	2.311

[a]Relative to Cr at the origin [b]Refer to Fig. 3 and Table 4

TABLE 9 Experimental and calculated electronic transition energies (cm^{-1}) for [Cr(dpt)(ida)]ClO_4 $2H_2O$

State	Exp	Calc.[a]
^2E_g	14330	14338
	14486	14496
$^2T_{1g}$	14620	14635
	15098	14888
	15326	15304
$^4T_{2g}$ (av)	20492	20434
$^4T_{1g}$ (av)	27624	27655

[a]Parameter values and estimated propagation uncertainties (cm^{-1}): $e_{\sigma 0}$, 7505 (6025); $e_{\pi 0}$, 1400 (163), $e_{\sigma N}$ (N21, ida), 7286 (4523); $e_{\sigma N1}$ (N11 and N13, dpt), 7427 (7973), $e_{\sigma N2}$ (N12, dpt), 6799 (7804), B, 771 (44); C, 2692 (114), α_T, 125 (fixed), ζ, 250 (fixed).

perturbations to the metal d orbital energies from each ligand at its exact position [13]. These perturbations are expressed in terms of angular overlap model (AOM) parameters e_σ and e_π for each ligand. The parameter e_σ represents the increase in energy that would be experienced by the d_{z^2} orbital from a ligand directly on the z axis, and e_π represents the increase in energy that would be experienced by the d_{xz} or d_{yz} orbital from a ligand on the z axis. The 5×5 one-electron ligand field potential matrix, $\langle d_i|V_{LF}|d_j\rangle$ is constructed by summing the contributions from each ligand [13].

The transition energies were evaluated within the 120 function manifold of d^3 electronic states. The secular determinant was constructed from the Hamiltonian

$$\mathscr{H} = V_{LF} + \sum_{i<j} e^2/r_{ij} + \zeta \sum_i l_i \cdot s_i + \alpha_T \sum_i l_i^2 + 2\alpha_T \sum_{i<j} l_i \cdot l_j \qquad (1)$$

which parameterizes the interelectronic repulsion in terms of the spherical Racah parameters B and C, plus the Trees correction, through the parameter α_T, and also includes spin–orbit coupling by means of the parameter ζ. The adjustable AOM parameters for $[Cr(dpt)(ida)]^+$ are $e_{\sigma 0}$ and $e_{\pi 0}$ for the carboxylate ligands, $e_{\sigma N}$ for the imino nitrogen of iminodiacetate, $e_{\sigma N1}$ for the primary amines in di(3-aminopropyl)amine, and $e_{\sigma N2}$ for the dpt secondary amine. The nitrogens, having just one lone pair, were assumed to have no π-bonding capability.

These nine parameters (five AOM parameters and B, C, α_T and ζ) form too large a set for the available experimental data, which consist of the five sharp-line $^4A_{2g} \rightarrow \{^2E_g, {}^2T_{1g}\}$ transitions, and the two broad-band transitions to the $^4T_{2g}$ and $^4T_{1g}$ states. Two parameters were therefore fixed: the spin–orbit coupling parameter ζ was set at 250 cm^{-1}, and the Trees parameter α_T was set at 125 cm^{-1}. The uncertainty in the spin–orbit coupling parameter is usually very large when fitting the spectra of low-symmetry complexes, and its actual value makes little difference [23]. The Trees parameter has a greater influence on the transition energies, but its effects on the sharp-line splittings, as opposed to the absolute transition energies, is very small. It was set to a value typical for Cr(III) complexes [23, 24].

Table 8 lists the Cartesian coordinates for the six atoms coordinated to the chromium, and also for the carbon atoms attached to the two oxygens. These are

TABLE 10. AOM parameters for related complexes (cm^{-1})

Parameter	$[Cr(en)_3]$[a]	$[Cr(tacn)_2]Cl_3$[b]	[Cr(tcta)][b]	$K_3[Cr(ox)_3]$[c]	$[Cr(dpt)(ida)]ClO_4$[d]
$e_{\sigma 0}$			7906	7110	7505
$e_{\pi 0}$			2042	1440	1400
$e_{\sigma N1}$	7591				7286 (ida)
					7427 (dpt)
$e_{\sigma N2}$		7721	7048		6799

[a]Ref 24. [b]Ref 27. [c]Ref. 28 [d]This work. Ligand abbreviations en, 1,2-diaminoethane; tacn, 1,4,7-triazacyclononane, tcta, 1,4,7-triazacyclononane-*N*,*N*′,*N*″-triacetate, ox, oxalate

necessary to establish the Cr–O–C plane, perpendicular to which the carboxylate oxygens are presumed to have one lone pair that can engage in π-bonding with the metal [13]. The Cartesian coordinates are centered on the chromium atom and have been rotated to maximize the projections of the coordinating atoms on an axis.

A least-squares optimization [25] to the experimental energies was performed, in which the sharp-line doublets (except for T_2) were weighted one hundred times more heavily than the quartets or the T_2 line. The resulting calculated transition energies are shown in Table 9. The parameter values are also given in Table 9 along with the uncertainties propagated [26] from the estimated experimental uncertainties of 100 cm^{-1} for the quartets and the T_2 line, and 3 cm^{-1} for the doublets. The propagation errors appear to be quite large (possibly because the experimental uncertainties were overestimated), but the parameter values are quite consistent with those observed in other chromium(III) complexes, as seen in Table 10.

In Table 10 the dpt secondary amine has a smaller value of e_σ than does the primary amine. This is contrary to expectation, since secondary amines are stronger bases, and it may indeed be a consequence of the propagation of experimental errors. In another study involving the di(3-aminopropyl) ligand, only an average value for the amines was used in the calculation for $[Cr(dpt)(glygly)]ClO_4$ [20], but that average of 7370 cm^{-1} for $e_{\sigma N}$ is reasonably similar to the weighted average of 7220 cm^{-1} for the dpt nitrogens in this work.

References

1 S.T. Chow and C.A. McAuliffe, *Prog Inorg Chem*, *19* (1975) 51.
2 P E Hoggard, *Inorg Chem*, *20* (1981) 415.
3 V Subramaniam and P.E. Hoggard, *Inorg Chim Acta*, *155* (1989) 161.
4 V. Subramaniam, K.-W. Lee, R.G Garvey and P.E Hoggard, *Polyhedron*, *7* (1988) 523
5 O. Kling and H.L Schlafer, *Z Anorg Allg Chem.*, *313* (1961) 188.
6 H.-H. Schmidtke and D. Garthoff, *Inorg Chim Acta*, *2* (1968) 357.
7 (a) D.A House and W.T Robinson, *Inorg Chim Acta*, *141* (1988) 211, (b) G.H Searle and D A House, *Aust J Chem*, *40* (1987) 361
8 N F. Curtis, R.W. Hay and Y M Curtis, *J Chem Soc A*, (1968) 182
9 V. Subramaniam, *Ph D Dissertation*, North Dakota State University, Fargo, ND, 1989.
10 J. A Weyh and R E. Hamm, *Inorg Chem*, *7* (1968) 2431.
11 N Koine, T. Tanigaki, J Hidaka and Y Shimura, *Chem Lett*, (1980) 871
12 S. Yano, M Watabe and S Yoshikawa, *Inorg. Nucl Chem Lett*, *14* (1978) 279.
13 P E. Hoggard, *Coord Chem Rev*, *70* (1986) 85.
14 P E. Hoggard and H.-H Schmidtke, *Ber Bunsenges. Phys Chem*, *76* (1972) 1013.
15 C.D. Flint and A.P. Matthews, *J Chem Soc, Faraday Trans. II*, *71* (1975) 1389
16 P. Main, S E. Fiske, G Germain, J P. Declerq and M.M. Woolfson, *MULTAN*, a system of computer programs of crystal structure determination from X-ray diffraction data, Universities of York, (UK) and Louvain, Belgium, 1980
17 K.E Gilbert, *PCMODEL Molecular Modeling Software*, Serena Software, Inc., Bloomington, IN, 1987
18 U Burkert and N.L Allinger, *Molecular Mechanics*, ACS Monograph 177, American Chemical Society, Washington, DC, 1982.
19 K. Nakamoto, *Infrared and Raman Spectra of Inorganic and Coordination Compounds*, Wiley-Interscience, New York, 3rd edn., 1978.
20 J.-H. Choi and P.E. Hoggard, *Polyhedron*, *11* (1992) 2399
21 Y. Yoshikawa and K Yamasaki, *Bull Chem Soc. Jpn*, *45* (1972) 179.
22 F A. Jurnak and K N Raymond, *Inorg Chem.*, *13* (1974) 2387.
23 K-W. Lee and P.E Hoggard, *Inorg. Chem*, *30* (1991) 264
24 P.E. Hoggard, *Inorg Chem*, *27* (1988) 3476
25 M.J.D. Powell, *Computer J*, *7* (1964) 155.
26 A.A. Clifford, *Multivariate Error Analysis*, Wiley-Halstad, New York, 1962
27 K.-W Lee and P E Hoggard, *Transition Met Chem*, *16* (1991) 377.
28 K.-W Lee, *Ph.D Dissertation*, North Dakota State University, Fargo, ND, 1989.